CHEMICAL ENGINEERING TRANSACTIONS
VOL. 51, 2016
A publication of AIDIC
The Italian Association of Chemical Engineering
Online at www.aidic.it/cet
Guest Editors: Tichun Wang, Hongyang Zhang, Lei Tian

ISBN 978-88-95608-43-3; **ISSN** 2283-9216
DOI: 10.3303/CET1651051

Microscopic Mechanism of Tin-Cobalt Alloy Negative Material During Li-Absorption

Yong Li[*a,b], Yuxin Zhang[a], Shiming Li[c], Jinmei Wu[a], Yaping Ding[d], Ruizhu Zhang[a]

[a]Dept.of Mechanical Engineering, North China University of Water Resources and Electric Power, Zhengzhou, 450046, China
[b]School of Materials Science and Engineer, Shanghai University, Shanghai, 200444, China
[c]Hebei Better Rubber Co., Ltd., Hengshui, 053100, China
[d]Department of Chemistry, Shanghai University, Shanghai, 200444, China
liyong@ncwu.edu.cn

This investigation calculated band structure, density of states, total charge density distribution and crystal performance of CoSn alloy anode embedding lithium, and examined the volume expansion and the formation energy. As well as the distinction of band structure of all alloys systems doped lithium atoms was discussed in comparison with CoSn alloy model. The results found that Li-absorption is feasible to generate new chemical bond with Sn atoms, but cannot combine with Co atoms associated with the higher inert chemically. Additionally, the study of volume expansion and formation energy doped lithium indicated that two lithium phases of $Li_2Co_3Sn_3$ and $Li_3Co_3Sn_3$ have the property of the smaller volume expansion, and the formation energy can be positive and low, which is beneficial for lithium and deintercalation, thereby improving cycle characteristics of CoSn alloy battery. Consequently, when 2-3 lithium is integrated in Co_3Sn_3 model, individuals may receive the best cycling performance and design new negative electrode material.

1. Introduction

As a relatively recent negative electrode material, two critical characteristics of CoSn alloys are excellent storage capacity and high performance of lithium (Jiang et al., 2004; Mi et al., 2003). Generally, Sn and Li can form an ultra-high-capacity with the intermetallic compound, and 1mol tin can accommodate 4.4 mol Li in the average. Additionally, its theoretical specific capacity is up to 990 mAh/g, and the value is more than twice than the graphite with theory capacity of 372 mAh/g (Tamura et al., 2004). Although there are many problems of microscopic mechanism, such as the gap may be formed of a variety of solid solutions between tin and cobalt (Guo et al, 2007; Guo et al., 2008). Less cyclical, and its disadvantages of cycle performance cannot be avoided. Therefore, the current work is concentrated on improving cycling property of tin-cobalt alloy anode materials and so on.

In recent years, calculations based on the density functional theory become increasingly distinguished by the first principle and molecular dynamics (Wang et al., 2015; Dawar et al., 2015; Monkhorst and Pack, 1976; Zhang and Chen, 2015; Li et al., 2016; Ravindran et al., 1998), which appear in designing and synthetic materials, simulation and evaluation. Therefore, it has become an indispensable research methods of developing materials, and the key is to study the relationship between structure and properties of materials (Shen et al., 2010; He et al., 2009). In addition, it noted that the volume effect of lithium battery anodes during charging and discharging and instability SEI film must be taken into account (Shieh et al., 2006; Dawar and Joshi, 1984; Dean, 2008), these behaviours can cause financially-challenged cycle performance of the electrode material. For these key issues, theoretical investigation of genetic material is proposed in fact of Li-doping mechanism from atoms and electrons structure of trans-scale (Hays et al., 2005; Lewis and Paine, 2000).

At present, tin-cobalt alloy electrode materials are more concerning on experimental basis value because of the test method (Giuseppeet al., 2016), and microscopic mechanism is restricted to the superficies of tin-cobalt alloy lithium, so that scholars are hard to take up the further study of pewter formidable performance

Please cite this article as: Li Y., Zhang Y.X., Li. S.M., Wu J.M., Ding Y.P., Zhang R.Z., 2016, Microscopic mechanism of tin-cobalt alloy negative material during li-absorption, Chemical Engineering Transactions, 51, 301-306 DOI:10.3303/CET1651051

lithium. Residential study found the presence of a large volume change issues as a lithium-ion battery anode material metal tin (Hohenberg and Kohn, 1964; Segall et al., 2002; Giuseppe et al., 2016), which leads to limited applications of space metallic tin-anode materials for lithium batteries, and it is necessary to understand the microscopic mechanism of tin metal anode materials for lithium storage.

Therefore, this work built a few of CoSn alloys models using Material Studio (Segall et al., 2002), then engaged in calculation of CoSn lithium and structural optimization by first-principles and pseudopotential plane wave method, further to acquire band structure, density of states (DOS), lithium formation energy and volume expansion of CoSn lithium, in order to identify more appropriate as a lithium negative electrode material phase, which provides useful guidance as a practical application for the CoSn alloy anode materials.

2. Computational Details and Methods

2.1 Crystal Structure

CoSn crystal model is showed in Figure 1a, it belongs to the hexagonal system (Jain et al., 1972 and, Mao and Dahn, 1999), and the space group structure is P6/mmm, or code-named of the space group is 191, and the lattice constant is a=b=5.279 Å, c=4.259 Å. In the light of specific gap location, such as body-centered, face-centered and so on, these special positions are most likely to be close to the position where the lithium atoms are optimization. Moreover, lithium ions preferentially occupy interstitial lattice positions during embedding lithium, and locate in the larger gap position. As shown in Figure 1b, the site between the two Sn atoms on the border has a large gap, thus lithiums doped firstly occupy the space between two atoms of Sn1, then name $Li_xCo_3Sn_3$ (x=1-8). With the intercalation of lithium ions is continued, as shown in Figure 1b. In order to ultimately develop the most suitable lithium model as the negative electrode material, and so as to better promote the practical application of tin compounds with inter-cobalt metal as anode materials.

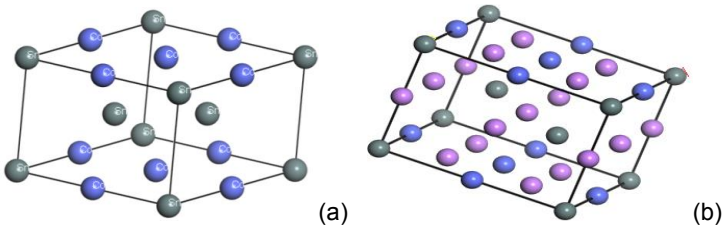

Figure 1: Crystal models (a)-CoSn, (b)-$Li_8Co_3Sn_3$

2.2 Computational Methods

The calculation firstly optimized structural model by first-principles (Triki and Ezzeddine, 2008), and then set the appropriate parameters, including density approximation function and plane wave basis set extensions in the framework, and the exchange-correlation part is described with generalized gradient approximation (GGA) (Perdew et al., 1993) and Perdew-Wang' 91(PW91) (Mishra and Ceder, 1999; Hammer et al., 1999), and also the exchange-correlation function was used to describe under the spin-polarized. Taking account of calculation convergence, interatomic force is less than 0.05 $eVnm^{-1}$, and the maximum forces on each relaxed atom is less than 2×10^{-5} eV. Respectively, internal stress is lower than 0.05eV/Å. In order to make the most stable local structure, the work is prior to the operation of the lattice parameters and the atomic position fully relaxed through Broyden Flecher Goldfarb Shanno (BFGS) method. According to the Monkhorst-Pack scheme (Monkhorst et al., 1976) k-point mesh with 6×6×8 (For unit cell cases) used for the integration of the Brillouin zone, energy calculate in reciprocal space under the condition of periodic boundary conditions. Cut-off Energy for convergence is chosen to 360eV.

3. Results and Discussion

3.1 Band Structure, DOS and Charge Distribution

Figures 2a and 2b are respectively band structure diagram of CoSn and Li8Co3Sn3 alloys. Noted that the part below the Fermi level is very flat and dense because of amount of atoms. Therefore, the resulting of energy band diagram still can be indicated that there are conduction band or valence band crossing the Fermi level in Figure 2, so the both models belongs to metallic. Compared with CoSn, the range of Li1Co3Sn3 energy band is narrower, and its curve becomes flat, and it exhibits ionic. The results further demonstrate that this change is related to the newly added lithium atoms, and they occurs charge transfer. At the same time, one separate band is can see in -47.6 eV place, which is caused by 1s electronic of lithium atoms, and indicates that new chemical bonds are formed while embedding between lithium atoms and tin atoms. Figure 2b shows that

Li8Co3Sn3 alloy exhibits stronger ionic than the other models with embedding lithium atoms. Although energy band diagram of $Li_xCo_3Sn_3$ (x=1~7) alloys is very similar, and has relatively narrow band range. Similarly, the emergence of a number of separate band is in -47.4 eV place, and still appeared wide black line. With increasing number of lithium intercalation, the separation zone will gradually increases, which is caused by the valence electrons of the doping amount of lithium increases sake.

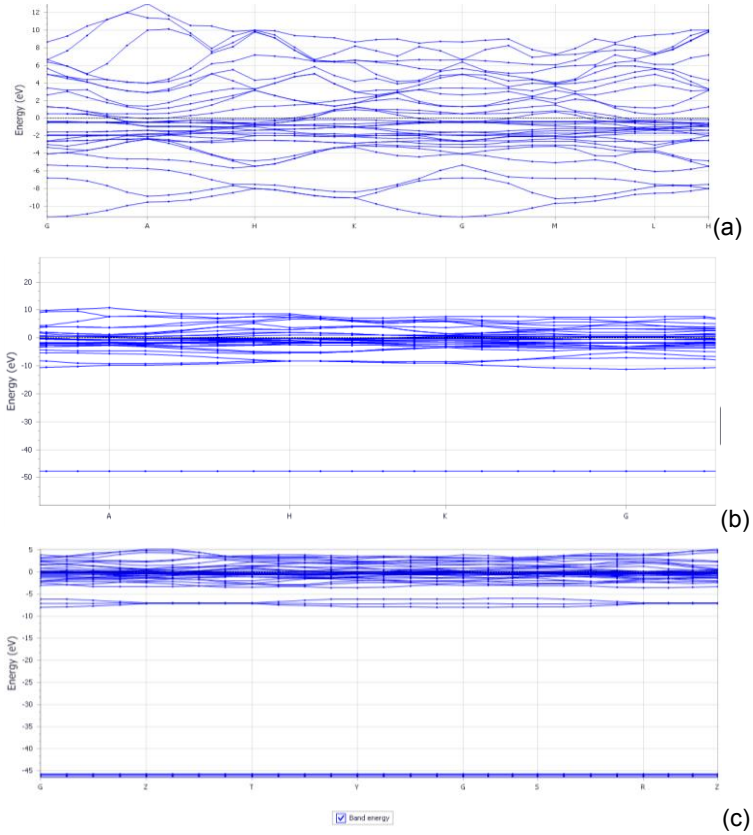

Figure 2: Band structure (a)-CoSn, (b) $Li_1Co_3Sn_3$, (c)-$Li_8Co_3Sn_3$

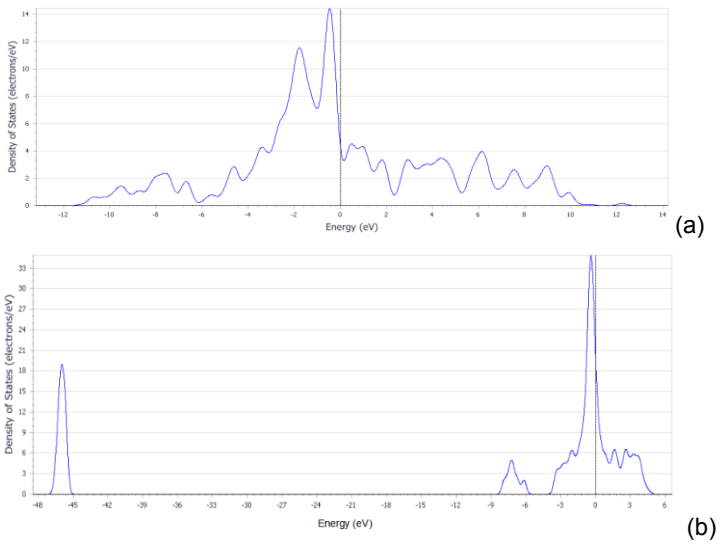

Figure 3: Crystal density of states (a)-CoSn, (b)-$Li_8Co_3Sn_3$

Figure 3a and 3b is the density of total states of CoSn and $Li_8Co_3Sn_3$ alloys, and the second curve demonstrates that the curve shape appears at -45.9 eV, which consistent with band structure calculations.

Obviously, the density of states of all sub-models has partial wave DOS across the Fermi level, and all alloys models exhibit metallic. In addition, Co (3d) determines the total electron density of states, because the lithium is doped into alloys and Fermi level near the line leads to the tin atom fractions, which occurs density change map and is consistent with other calculations of the band structure of lithium inlay. Consequently, it can be seen for all models, Co atoms severely impact on its total cobalt atom density of states, and lithium atoms are embedded into alloys impact on not only PDOS of tin atoms but also total DOS. Which indicates that 1s electrons play the key role in bonding areas while embedding lithium ions into alloys system.
According to Figure 4a and 4b, the charge distribution around the cobalt atom is less, which further describes the inert of cobalt is strong in this system. Figure 4c and 4d show electronics distributing around tin increase after intercalation of lithium, which indicates that lithium impacts on charge distribution of tin. But comparing the slender changes of charge distribution around the cobalt, lithium scarcely impacts on cobalt. Furthermore, lithium atoms litigated affect the charge distribution around tin when embedded in lithium, and four corners of the tin atoms around have not intersection, which illustrates that lithium-ion embedded particularly forms a bond with tin.

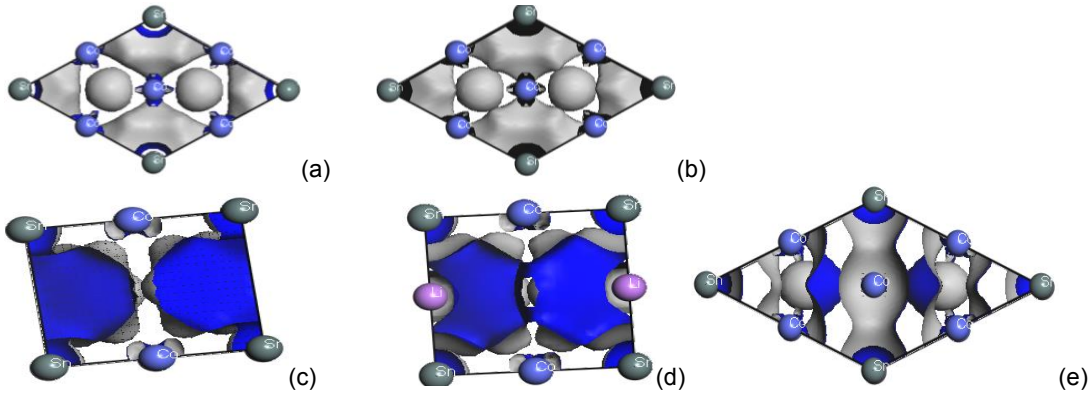

Figure 4: The total charge density distribution (a)(b)(e)-(0,0,1), (c)(d)-(0,1,0), (a)(c)-before intercalation, (b)(d)(e)-behind intercalation, (a~d)-one lithium embedded, (e)-two lithiums embedded

3.2 Formation Energy

Table 1 mainfests lattice parameters and cell volume of $Li_xCo_3Sn_3$, and lists the intialvalue and optimization of bonds length and volume. Manifestly, overall volume is increased, beside $Li_xCo_3Sn_3$ (x=3-7) appear irregular movement, and the most important cause of inordinance is related to the change of lattice constant and the location of the lithium ions into the body-centered position. If lithium is inserted in the frame, and the corresponding lattice constant becomes bigger. Additionally, calculation results reveal the changed bond angle of different unit cell during lithium insertion process. So far as to directly transfer hexagonal crystal into the normal tetragonal composed, which shows that the structures of the whole system significantly change because of intercalation.

Table 1: lattice parameters and cell volumen (Xie et al., 2006; Zhang and Xia, 2006)

Parameters	Experiment	A (Å)	B (Å)	C (Å)	V (Å^3)
Sn_3Co_3	Initialvalue	5.279	5.279	4.259	102.788
	optimized	5.411	5.411	4.324	126.602
$Li_1Co_3Sn_3$	optimized	5.401	5.401	4.613	134.565
$Li_2Co_3Sn_3$	optimized	6.152	6.152	4.702	177.957
$Li_3Co_3Sn_3$	optimized	5.985	5.985	4.769	170.827
$Li_4Co_3Sn_3$	optimized	7.260	7.260	4.702	247.831
$Li_5Co_3Sn_3$	optimized	7.941	7.941	4.668	294.362
$Li_6Co_3Sn_3$	optimized	7.024	7.024	4.738	233.757
$Li_7Co_3Sn_3$	optimized	7.309	7.309	4.966	265.291
$Li_8Co_3Sn_3$	optimized	7.368	7.368	5.230	283.923

Generally, cycle performance of lithium-ion battery anode material can be lower due to the volume expansion, and formation energy represents the difficulty of lithium embedded and deintercalation. If energy value is negative, lithium difficultly embeds, and once forms a relatively stable compound, right now, lithium is hard to

deintercalate. On the contrary, when the value is positive and smaller, the livelier phase is formed, and the reaction of intercalation and deintercalation easily occurs. The curve in Figure 5 shows the volumetric expansion of each model, when the insertion of lithium ions becomes sustained growth, and volume expansion is increasing in proportion. Especially, volume $Li_8Co_3Sn_3$ model is bigger than Co_3Sn_3, which is an important cause of underdeveloped circulation of Co_3Sn_3 as the negative electrode material.

Accordingly, the energy of the ideal electrode material must be positive and the value is lower. After comparative calculation of six lithium models, formation energy of $Li_1Co_3Sn_3$ is negative. It indicates that the structure of CoSn alloy is relatively stable at the beginning of lithium, and deintercalation is formidable. As a result, this will result in a loss of lithium ions during charge and discharge and occur death phase of lithium. As shown in Figure 5, beside the $Li_1Co_3Sn_3$ phase, the formation energy of other lithium phases is positive, and the trend of growing energy is presented with increasing the embedded lithium. However, the energy condition is preferably negative and less. In consequence, intercalation phase of $Li_xCo_3Sn_3$ (x=2-4) can comply with the requirements.

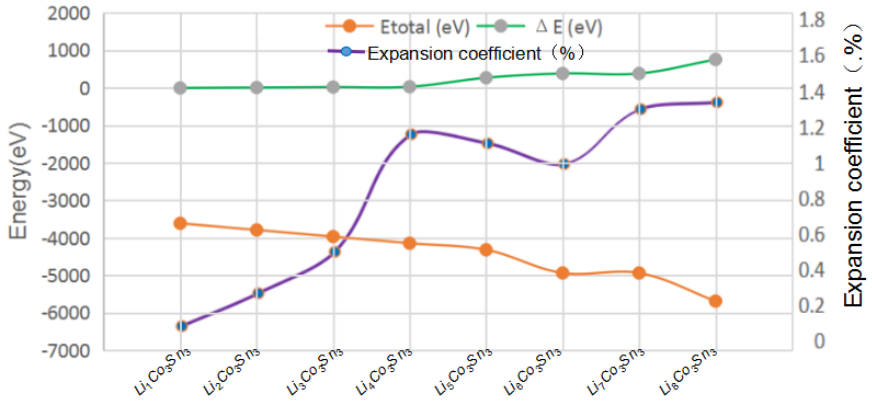

Figure 5: Formation energy and volume expansion coefficient of $Li_xCo_3Sn_3$

4. Conclusions

In summary, phenomenon of band intertwined and band crossed the Fermi level shows that CoSn alloy and lithium models belong metallic, and new bonds of Li-absorption gradually form with increasing the embedded lithium, which indicates that the conductive capacity of the entire system is enhanced after intercalation. Additionally, the whole system may occur overwhelmingly severe volume expansion while embedding 5-8 lithium, and qualified intercalation phases are $Li_xCo_3Sn_3$ (x=2-4), which identifies more appropriate as a lithium negative electrode material phase, and develop rewarding guidance as a practical application for the CoSn alloy anode materials.

Acknowledgments

This work was supported by the Higher key scientific research projects of Henan province in China (Grant No.17A460020) and the Ministry of water resources science and technology promotion project (Grant No.TG1420).

Reference

Dawar A.L., Jain A.K., Jagadish C., and Hartnagel H.L., 1995, Semiconducting Transparent Thin Films (Institute of Physics, London).

Dawar A.L., Joshi J.C., 1984, Semiconducting Transparent Thin Films: Their Properties and Applications, J. Mater. Sci., 19, 1-23, DOI: 10.1007/BF00552989.

Dean J.A. (ed.), 2008, Lange's Handbook of Chemistry, Fourteenthed, (McGraw-Hill, Inc., New York, 1992), 055502, DOI: http://dx.doi.org/10.1103/PhysRevLett.101.055502.

Giuseppe G., Federico M., Adriano M., 2016, Constructal Design of the Mixing Zone Inside a Supersonic Ejector, International Journal of Heat and Technology, 34(S1), S109-S118.

Guo Y.G., Hu J.S, Wan L.J., 2008, Nanostructured Materials for Electrochemical Energy Conversion and Storage Devices, Adv Mater, 20(15), 2878-2887, DOI: 10.1002/adma.200800627.

Guo H., Zhao H.L., Jia X.D., et al, 2007, A novel Micro-spherical CoSn2/Sn Alloy Composite as High Capacity Anode Materials for Li-ion Rechargeable Batteries, Electrochim Acta, 52(14), 4853-4857, DOI: 10.1016/j.electacta.2007.01.058.

He J.C., Zhao H.L., Jia X.D., et al., 2009, Research Progress of Sn-Co Anode Materials Forlithium-ion Batteries, CIESC J, 60(5), 1073-1079.

Hohenberg P., Kohn W., 1964, Inhomogeneous Electron Gas, Phys. Rev., 136, B864-B871.

Hays J., Punnoose A., Baldner R., Engelhard M.H., Peloquin J., Reddy K.M., 2005, Relationship between the Structural and Magnetic Properties of Co-doped SnO2 Nanoparticles, Physical Review, 72(7), 075203, DOI: http://dx.doi.org/10.1103/PhysRevB.72.075203.

Hammer B., Hansen L.B., Norskov J.K., 1999, Phys. Rev. B, 59, 7413-7421. DOI: htp://dx.doi.org/10.1103/PhysRevB.59.7413.

Jiang M., Sato J., Ohnuma I., Kainuma R., Ishida K., 2004, A Thermodynamic Assessment of the Co-Sn System, Calphad, 28(2), 213-220, DOI: 10.1016/j.calphad.2004.08.001.

Jain K.C., Ellner M., Schubert K., et al., 1972, On the Phases Occurring Near the Composition Cu64In36, Pre: B. Predel and U., 63, 456-461.

Li Y., Zhang Y.X., Kong X.R., et al., 2016, Investigation on Thermodynatic Performances of Mg2Sn Compound via First Principle Calculations, International Journal of Heat and Technology, 34(1), 110-114.

Lewis B.G., Paine D.C., 2000, Applications and Processing of Transparent Conducting Oxides, MRS Bull, 25(8), 22-27, DOI: http://dx.doi.org/10.1557/mrs2000.147 (About DOI).

Mi C.H., Zhang X.G., Cao G.S., 2003, Synthesis and Characteristics of Cosn and Cu-Sn Alloys as Anode Materials in Lithium-Ion Cell, Chinese Journal Of Inorganic Chemistry, 19(3), 283-286, DOI: 0.3321/j.issn:1001-4861.2003.03.011

Monkhorst H.J. and Pack J.D., 1976, Special points for Brillouin-zone integrations, Phys. Rev. B: Condens. Matter Mater. Phys., 12, 5188, DOI: http://dx.doi.org/10.1103/PhysRevB.13.5188.

Mao O., Dahn J. R., 1999, Mechanically Alloyed Sn-Fe(-C) Powders as Anode Materials for Li-Ion Batteries System, Journal of The Electrochemical Society, 146(2), 414-422.

Mishra S.K., Ceder G., 1999, Structural Stability of Lithium Manganese Oxides, Physical Review B, 59(9), 6120-6130, DOI: http://dx.doi.org/10.1103/PhysRevB.59.6120.

Perdew J.P., Chevary J.A., Vosko S.H., 1993, Physical Review B, 46(11), 6671-6687, DOI: http://dx.doi.org/10.1103/PhysRevB.46.6671.

Ravindran P., Fast L., Korzhavyi P.A., Johansson B., Wills J., Eriksson O., 1998, J. Appl. Phys., 84 4891, DOI: http://dx.doi.org/10.1063/1.368733.

Shen D., Yang S.B., Yang F., et al., 2010, Synthesis and Lithium Storage Performance of Sn-Co Alloys by Solid-state Sintering Method, Chinese J Power Sources, 34(4), 371

Shieh S.R., Kubo A., Daffy T.S., Prakapenka V.B., Shen G.Y., 2006, High-pressure phases in SnO2 to 117 GPa, Phys. Rev. B, 73, 014105, DOI:http://dx.doi.org/10.1103/PhysRevB.73.014105.

Segall M.D., Payne J.M., Lindan C., et al., 2002, First-principles Simulation: Ideas, Illustrations and the CASTEP Code, Phys.:Cond. Matt., 14(11), 2717-2743.

Tamura N., Fujimoto A., KaminoM et al., 2004, Mechanical Stability of Sn-Co Alloy Anodes for Lithium Secondary Batteries, Electrochimica Acta, 2004. 49(12), 1949-1956, DOI: 10.1016/j.electacta.2003.12.024.

Triki Ali, Ezzeddine H.T., 2008, Numerical Simulation for One Dimensional Open Channel Transient Flow, International Journal of Heat and Technology, 26(1), 89-96.

Wang J.T., Yu W.L., Gao Y.L., 2015, First-principles Study on the Thermodynamic Defect and Crystal Structure of U-12.5 At% Nb Alloy, International Journal of Heat and Technology, 33(1), 175-180.

Xie J., Zhao X.B., Yu H.M., et al., 2006, Preparation, Characterization and Electrochemical Li-absorption/Extraction Behaviors of Nanosized Co-Sn Inter-metallic Compounds, Acta Phys-Chim Sin, 22(11), 1409-1412, DOI: 10.3866/PKU.WHXB20061120.

Zhang, S., Chen, L.S., 2015, Semiconductor, Molecular Crystals and Oxide Temperature Pressure Ophase Diagram, International Journal of Heat and Technology, 33(1), 123-128, DOI: 10.1002/adfm.200600431.

Zhang J.J., Xia Y.Y. , 2006, CoSn Alloys as Negative Electrode Materials for Lithium-ion Batteries, Chem J Chinese University, 10(27), 1923-1926, DOI: 10.3321/j.issn:0251-0790.2006.10.024.